

Application of silicon micro hall sensors in variable temperature scanning hall probe microscopy (SHPM) using multiple feedback techniques

Rizwan Akram *

Faculty of Electrical Engineering, Qassim University, P. O. B. 6677, Buraidah, 51452, Saudi Arabia

ARTICLE INFO

Article history:

Received 30 December 2017

Received in revised form

24 March 2018

Accepted 8 April 2018

Keywords:

Hall effect devices

Scanning hall probe microscopy

Silicon on insulator

Quartz tuning fork

Atomic force microscopy

Scanning tunneling microscopy

ABSTRACT

A quest for a quantitative and noninvasive method for the measurement of local magnetic fields along with surface morphology with high spatial and field resolution at variable temperatures calls for a selection of suitable magnetic sensor and appropriate scanning system. Scanning Hall probe microscopy (SHPM) is one of the choices as it addresses the stated issues and complements the other magnetic imaging methods. Si-Hall sensors due to their compatibility with CMOS technology and controllability of its parameters makes it preferable compared to other compound semiconductors. However, there have been few reports on magnetic imaging with Si-Hall sensors at high-temperatures and the selection of best possible feedback mechanism for them has not been addressed. In this article, working temperature range and the impediments related to feedback (STM tracking or AFM tracking) configuration for Si-Hall sensors along with feasibility of switchable feedback tracking configuration has been investigated. Si-Hall sensors ($\sim 0.7\mu\text{m} \times 0.7\mu\text{m} \times 510\text{nm}$) have been fabricated with integrated Gold tip for STM-feedback and were mounted on Quartz Tuning Fork (QTF) for AFM-feedback. Comparison of simultaneous scans of magnetic and topographic data for a Hard disc sample, illustrated that the Si-Hall sensors are capable of scanning with comparable quality of images as with AlGaAs-HP for low temperatures (down to LNT) using STM feedback and as GaN/AlGaN-HP for high temperatures up to 150oC using AFM feedback. Use of QTF with Si-HP provided an option to electronically switch the feedback configuration between STM and AFM without the need to change front end assembly.

© 2018 The Authors. Published by IASE. This is an open access article under the CC BY-NC-ND license (<http://creativecommons.org/licenses/by-nc-nd/4.0/>).

1. Introduction

Hall sensors are widely used in various applications ranging from high-end industrial and scientific research applications to everyday solutions. Further, micro-Hall sensors have also been used for novel applications including scanning Hall probe microscopy (SHPM) of ferromagnetic domains (Oral et al., 1996; Schweinböck et al., 2000) and as biosensors for the detection of superparamagnetic particles for biorecognition (Mihajlović et al., 2005; Kumagai et al., 2008; Xiao-Fen et al., 2016; Karci et al., 2014). Scanning Hall probe microscopy (SHPM) has been demonstrated as one of the best choices as it provides adequate means to perform sensitive, noninvasive, and quantitative imaging for the

investigation of localized surface magnetic field fluctuation at variable temperatures with high spatial resolution and for non-metallic samples. SHPM technique offers various advantages and complements the other magnetic imaging methods like Scanning Superconducting Quantum Interference Device Microscopy (SSM) (Kirtley and Wikswo, 1999), Magnetic Force Microscopy (MFM) (Martin and Wickramasinghe, 1987), Magnetic Near-Field Scanning Optical Microscopy (Betzig et al., 1992) and Kerr Microscopy (Schmidt and Hubert, 1986). However, there have been few reports on magnetic imaging with Hall sensors at high-temperature regime too (Yamamura et al., 2006; Akram et al., 2008). Scanning Hall Probe Microscopy (SHPM) has been demonstrated as a quantitative and non-invasive technique for imaging localized surface magnetic field fluctuations of ferromagnetic domains with high spatial and magnetic field resolution of $\sim 50\text{ nm}$ and $7\text{ mG/Hz}^{1/2}$ at room temperature (Sandhu et al., 2004).

* Corresponding Author.

Email Address: rizwanakram75@qec.edu.sa<https://doi.org/10.21833/ijaas.2018.06.011>

2313-626X/© 2018 The Authors. Published by IASE.

This is an open access article under the CC BY-NC-ND license

(<http://creativecommons.org/licenses/by-nc-nd/4.0/>)

For applications like the characterization of magnetic properties of biological samples and magnetic materials, high sensitivity is essential. Magnetic detection levels are the key concern about the selection of the method used for such characteristics. Superconducting Quantum Interference Devices (SQUID) has the highest level of magnetic sensitivity, 5×10^{-18} T, among the local probing techniques (Oral et al., 1996; Akram et al., 2006). However, SQUID can only operate under cryogenic temperatures, which is the major drawback for their applications. Thus, when flexibility is needed in terms of the temperature, the best choice becomes the Hall devices again. To compete with other magnetic local microscopy techniques, the required modifications are required to circumvent the limitations associated with the detection capability of the Hall sensors. Absolute magnetic sensitivity and the noise levels are the two most important parameters that influence the sensitivity of the overall system (Kunets et al., 2005).

Silicon has been identified as one of the materials for the fabrication of sensors as it is the most established semiconductor technology. On the other hand, some specific problems are there in silicon Hall sensors. For instance, due to piezoresistive nature of Silicon, under stress piezoresistive voltage signals in Si Hall sensors may possess higher voltage levels than magnetic Hall voltages (Gruger et al., 2006; Chung, 1993; Paun, 2016). Besides, another problem associated with silicon Hall sensor magnetometer's is its offset, which becomes more important when it drifts. Normally the perfect Hall sensor should not have any output voltage in the absence of magnetic field. However, in practical situations, all Hall sensors have offset voltage due to the various factors like; material inhomogeneity, the constructional defects of the sensor, mechanical stresses, temperature variations and aging (Bellekom and Sarro, 1998; Paun et al., 2014; Paun et al., 2013a;b). The use of silicon on insulator (SOI) technology has been shown to contribute positively to improve offset reduction (Paun et al., 2014; Blagojevic et al., 2006a;b). One of the major advantages of SOI technology beside this is the use of insulated thin silicon layer instead of the whole silicon substrate in the fabrication of Hall sensors. It has been shown that this leads to a higher current density in the active Hall element and a reduction in the level of piezoresistive effect (Gruger et al., 2006).

Although in literature, a considerable number of papers regarding the fabrication of Si Hall probes and their application (Sandhu et al., 2004; Besse et al., 2002; Boero et al., 2005; Boero et al., 2003; Kejik et al., 2006) are available but these articles have mainly aimed to consider the fabrication of Hall sensors with dimension down to few tens of micrometer. As the size of the Hall sensors plays a very important role for their dedicated applications, therefore recently a thorough study on the effect of Si device layer thickness with respect to a different biasing parameter (Biasing current, Temperature,

etc.) has been completed and is submitted for publication.

These Hall Effect sensors can be integrated in scanning Hall probe microscope using different modes of feedback configurations in order to keep the Hall sensor in close proximity of the sample surface (Julian, 2014). Although there are other methods like integrating Hall sensor with piezoresistive (Paun et al., 2014) and Si_3N_4 AFM cantilevers (Chong et al., 2001) for better resolution, however, it is relatively difficult and cumbersome to micro fabricate conventional 2DEG hetero-structure (GaAs, InGaAs, InAs, InSb, AlGaIn/GaN) Hall sensors and integrate them in these complicated configurations. Whereas Si Hall probes can handle the difficulties related to the fabrication due to being CMOS compatible (Gruger et al., 2006; Paun et al., 2016). In this study application of SHPM technique, scanning tunneling microscope (STM) or atomic force microscope (AFM) feedback is used (Julian, 2014).

However, there have been few reports (Yamamura et al., 2006) on magnetic imaging with Hall sensors in the high-temperature regime. The main reason behind the unsuitability of SHPM at high temperatures is the use of compound semiconductors such as AlGaAs/GaAs and InSb for fabrication of Hall probes, which are unstable at elevated temperatures due to their narrow bandgap and physical degradation of the material. Recent work on AlGaIn/GaN hetero structures shows a stable high-temperature application in SHPM, but as stated above integration of these materials with AFM cantilever is cumbersome and hard.

In this study an application of Si sub-micron ($\sim 0.7 \mu\text{m} \times 0.7 \mu\text{m}$) Hall sensors with optimized thickness, 510nm, in variable temperature SHPM system have investigated using two main feedback techniques, STM and AFM (using quartz crystal tuning fork (QTF) sensor (Guethner et al., 1989; Akram et al., 2008). The focus has been to explore the bottlenecks associated with each method for their use at variable temperature applications of Si based SHPM.

2. Device fabrication and characterization

In the classical approach, the Hall cell is shaped like a Greek cross. The structure has some symmetry and it is invariant by a rotation of $\pi/2$. This allows the current-spinning technique to be used for minimizing residual offsets.

The Hall cross presented in Fig. 1, has four contacts (in darker grey shades), among which two perpendicular contacts are used to impose a current and others are used for sensing the Hall voltage. Length and width of the cross are respectively denoted by 'l' and 'w' and the thickness of the active region is referred as t_{eff} . The size of the Hall sensors plays very important role for their dedicated applications, where high spatial resolution is required, therefore more efforts are required in this direction to reduce the size of Hall sensors.

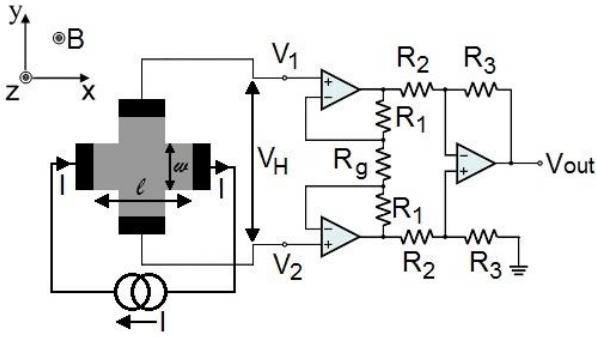


Fig. 1: Schematic diagram for characterization and use of Hall Effect sensor in scanning Hall probe microscopy system

According to device physics if a Hall sensor is placed in a static magnetic field $\mathbf{B} = B\hat{z}$, a Hall voltage appears between the sense contacts and can be written as;

$$V_H(B) = \frac{Gr_H}{nqt_{eff}} I_H B = \frac{R_H I_H B}{t_{eff}}, \quad (1)$$

where I_H is the biasing current, r_H is the scattering factor of silicon that can be approximated to 1.15, n is the carrier density, q is the magnitude of the electron charge, t_{eff} is the thickness of the plate (Paun et al., 2010). G is the magneto-geometrical factor and can be calculated as,

$$G = 1 - 5.0267 \frac{\theta_H}{\tan(\theta_H)} e^{-\frac{\pi}{2} \frac{w+2l}{w}}, \quad (2)$$

where $\theta_H = \tan^{-1}(\mu_H B)$, defined as the Hall angle (Xu and pan, 2011) and μ_H ($\mu_H = r_H \mu_n$) is the Hall mobility, and μ_n is the electron mobility.

The absolute sensitivity of Hall Effect sensor is given by

$$S = \frac{V_H}{B} = \frac{Gr_H}{nqt_{eff}} I_H = GS_I I_H, \quad (3)$$

where S_I is the current related sensitivity. S_I can be calculated from Hall coefficient, R_H , as $R_H \triangleq -\frac{1}{nq}$ (Xu et al., 2011; Popovic, 2004; Lyu et al., 2015; Boero et al., 2003).

As derived in (3) under constant current supply mode, sensitivity, S , of Hall devices can be enhanced by having high electron mobility and an ultra-thin device layer very close to the material's surface. Therefore, the development of the Hall devices requires new materials for the fabrication of highly sensitive sensing elements with an appropriate thickness to keep the aspect ratio. Along with this a growing interest in room temperature and elevated temperature applications of Hall sensor technology require the development of materials exhibiting high electron mobility and ultrathin conducting layers close to the material's surface (Abderrahmane et al., 2012).

From parametric equations (1-3), it can be concluded that the important physical parameters, which defines the characteristics of Hall device, are

carrier density, length of Hall device, width of Hall device, effective thickness of Hall cross, operating temperature, geometrical factor and bias current. In the previous study fixed length/width ratio of '1' has been used which fixes the geometry based variables for the Hall Effect device. The main focus has been to investigate the effect of t_{eff} , I_H and the operating temperature on selected characterizes of the Si Hall probes.

2.1. Hall effect sensor fabrication

SOI wafers from University Wafer, with n-type device and p-type handle layer as shown in Fig. 2a, are used for fabrication of $0.7\mu\text{m} \times 0.7\mu\text{m}$ Hall sensors Fig. 2b.

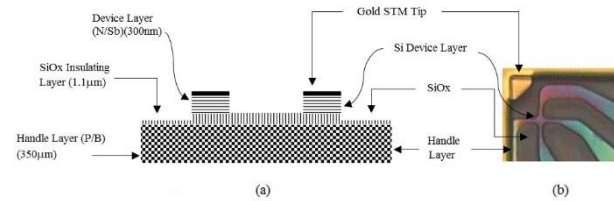


Fig. 2: (a) Schematic diagram of the layer configuration of the SOI Hall probe, (b) Photograph of $0.7\mu\text{m} \times 0.7\mu\text{m}$ Hall probe

These Hall probes are fabricated in class 100 clean room environments by using optimized photolithographic technique. These Hall sensors are micro-fabricated on $5\text{mm} \times 5\text{mm}$ chip in the form of four. These Hall sensors are later diced to a size of $1\text{mm} \times 1\text{mm} \times 0.5\text{mm}$ to be characterized and to be used in SHPM application (Akram et al., 2009). Electrical connections have been established with $12\mu\text{m}$ gold wire using ultrasonic wedge bonder. Furthermore, a gold tip is evaporated at the corner of the tip to provide access for STM tracking to be discussed later.

2.2. Hall effect sensor characterization

Device characterization for the dependence of Hall voltage, Hall coefficient, and noise has been investigated thoroughly for their dependence on temperature, device thickness and bias current and is presented somewhere else. The typical I_H vs. V_H and I_H vs. R_H characteristics curve at 25°C and 150°C for a device thickness of 510nm is shown in Fig. 3.

The observed linear behavior of these characteristics can be categorized in two different regimes; i) low current regime ($I_H \leq 100\mu\text{A}$) and ii) high current regime ($I_H \geq 100\mu\text{A}$). At any particular bias current, Hall voltage decreases by increasing the increasing temperature. Similar behavior has been observed for different device thicknesses as shown in Fig. 4.

In the previous reports, it has been speculated that the characteristics of these devices are strongly affected from the surface morphology of the thin film which is very much effect by the reactive ion etching process.

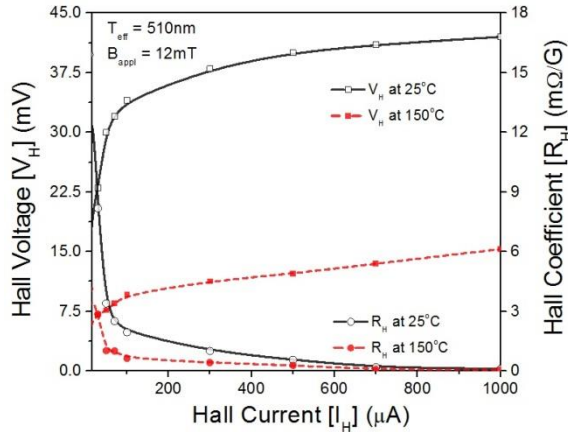


Fig. 3: Typical I_B vs. V_H and I_B vs. R_H characteristics of the SOI, 510nm thick and $0.75 \times 0.75 \mu\text{m}^2$ Hall Effect sensor characterized at 25°C

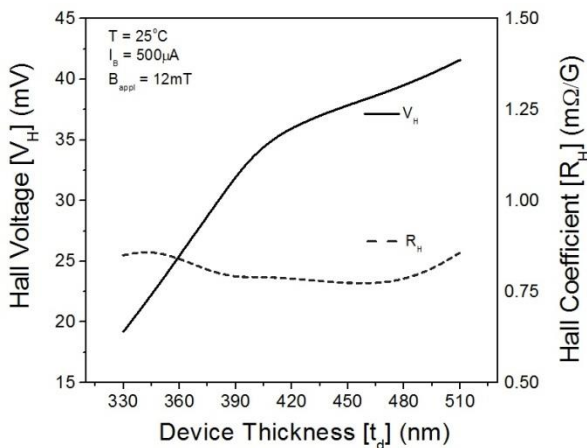


Fig. 4: Effect of device thickness on V_H vs. B_{appl} for $0.7 \mu\text{m} \times 0.7 \mu\text{m}$ Hall probe at 25°C at a fixed bias current of $500 \mu\text{A}$

3. Scanning hall probe microscopy

In order to demonstrate the feasibility of using these Si-Hall probes in SHPM and effect of feedback mechanism, low noise, and high SNR probe has been selected among the above discussed probes to be 510nm. Hall probes were operated in a current biased configuration having bias current of $500 \mu\text{A}$. The series resistance of the Hall sensor was $139\text{k}\Omega$, $144\text{k}\Omega$, $148\text{k}\Omega$, $152\text{k}\Omega$ and $157\text{k}\Omega$ at 25°C , 50°C , 75°C , 100°C and 150°C respectively. A commercial Low Temperature - SHPM system (NanoMagnetics) as shown in Fig. 5a is used to perform the scanning experiments. There were two main modifications, which was implemented in this system;

- 1) A local sample heating system has been integrated in the front-end assembly with a proper electrical and thermal insulation from sensor feedback and signal system.
- 2) Make it configurable to operate in different feedback tracking configurations.

3.1. Integration of Hall effect sensor in SHPM

As scanning probe techniques employ a feedback loop to facilitate keeping a constant interaction between the sensor and the sample as the sensor

scans the surface. In this study, the best possible feedback technique has been investigated for the use of Si-Hall Effect in variable temperature SHPM. In this regard, two different kinds of feedback configurations were compared, based on their best working range, namely conventional scanning tunneling (STM) feedback and novel AFM feedback using Quartz Crystal tuning fork.

In STM mode in Situ fabricated STM gold tip at the corner of the Hall probe is used to set tunneling current, which is used as a feedback to control the sample to sensor distance at a constant height. However, STM tracking SHPM requires conductive or semiconducting samples; therefore, the insulating sample has to be coated with a thin layer of gold (conductive material) as well. Furthermore, in order to simulate a sharp STM tip, the Hall probe assembly has been tilted by $\sim 1^\circ - 2^\circ$ so that sharp tip constraint can be resolved, as shown in Fig. 5b.

In AFM feedback as the sensor approaches the surface, the resonant frequency of the sensor shifts due to tip-sample forces. The sensor assembly is dithered at the resonance frequency with the dedicated split section of the scan piezo tube using a digital Phase Locked Loop (PLL) circuit. The frequency shift Δf , measured by the PLL circuit is used for AFM feedback to keep the sensor sample separation constant with the feedback loop as shown in Fig. 5c.

3.1.1. Front-end assembly for STM feedback

In order to investigate the effectiveness of scanning tunneling feedback method in Scanning Si-Hall Probe Microscopy, a 50nm gold tip, to establish tunneling current between sample and sensor, has been evaporated at the corner of Mesa step as shown in Fig. 6a.

In these experiments, STM tracking was done using a tunnel current of 0.5nA . In order to set this tunneling current to 0.5nA , a bias voltage of -0.1V has been applied between the tip and the sample. The front-end assembly of the probe installation in STM modes is shown in Fig. 6b. In order to measure tunnel current and Hall probe signals electrical connections were made by using wire bonding between tip metallization pad and interface PCB. In order to simulate a sharp tip, for proper tunneling, the corner of the Hall probe has been tilted with respect to sample as shown in the photograph of tip and sample angle in Fig. 6c.

3.1.2. Front-end assembly for AFM feedback

As STM tip is formed on the corner of Hall probe using gold thin film, which is prone to wear off easily and damage to Hall sensor follow inevitably and we need a conductive sample, these constraints can be eliminated with AFM feedback.

AFM feedback can be achieved either by integrating micro-Hall probes with AFM cantilevers (conventional) or by Quartz Tuning Fork, QTF force sensor. As fabrication of Hall probe on cantilevers is

The microscope can be operated in two modes: AFM tracking and lift-off mode. In our scanning experiments, we have used an AFM tracking mode with a Δf (amount of frequency shift) = 10Hz. We are bound to use contact wires, which affects the resonance frequency, but as we are sensing the shift of frequency during our scan, it does not cause an adverse effect. Furthermore, the same system can detect AFM topography and the phase signal generated by the PLL at the same time.

3.2. Scanning results and discussion

We have imaged magnetic bits and topography of the hard disc drive, HDD, at variable temperatures to show the performance of the microscope at variable temperatures and the impediments related to both stated feedback techniques.

3.2.1. Effect of scanning FB techniques

At low-temperature STM, tracking feedback produce a way better result compared to QTF-AFM technique as shown in Fig. 9a and 9b. While scanned Images at room temperature are of comparable quality as shown in Fig. 9c-9d. Therefore, it can be concluded that for low temperature to room temperature application STM tracking feedback can be applied if the sample can be coated with conductive material.

Scanning Hall probe microscopy also provides means to record the surface morphology simultaneously while recording the magnetic image by recording the 'z' position of the sample while keeping the constant height in STM and AFM tracking mode. The images show the comparable quality of the surface morphology of the sample, Fig. 9e and 9f.

3.2.2. Effect of temperature

At high temperatures use of STM, tracking feedback is effected by two main factors, 1) High leakage current between STM tip and Hall sensor and, 2) deterioration of the STM tip with temperature. Due to these reasons in this study, the max operational temperature achieved by STM feedback was 50°C and crashing of the sensor even does not allow the complete scan. So in order to compensate the drawbacks of STM feedback, QTF-AFM feedback has opted for high temperatures SHPM. Whereas a comprehensive study of theoretical modeling and experimental results on the characteristics of QTF AFM are presented somewhere else (Akram et al., 2008). In order to investigate the high-temperature operation of these Si micro-Hall probes, a low noise heater stage has been embedded in the LT system.

By increasing the temperature the resonance frequency and quality factor of the quartz crystal tuning fork are also affected as shown in Fig. 10. This slight shift in the resonance peak due to the effect of

temperature can be correlated with the softness of the glue used to fix one prong of the QTF with PCB and the corrosion of gluing Hall sensor chip to QTF.

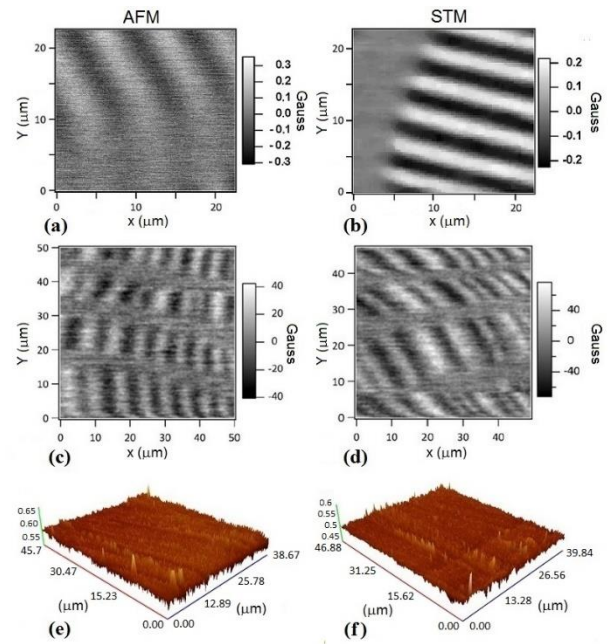


Fig. 9: SHPM image of hard disc sample using scanning speed was 5µm/s. QTF AFM (a) and STM (b) feedback at liquid Nitrogen temperature, (c) and (d) are scan results at 25°C, (e) and (f) are the surface morphology images recorded simultaneously

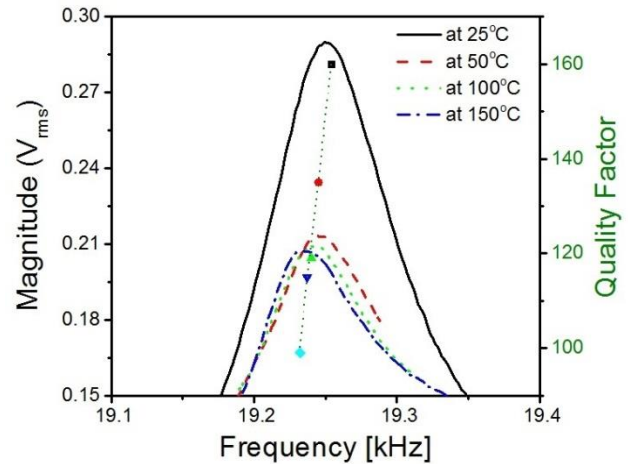


Fig. 10: Effect of Temperature on resonance frequency of the quartz tuning fork and quality factor

However, this change is still much less than the conventional silicon AFM cantilevers. Further investigation is under process to find out the methods to improve the thermal stability of the QTF AFM feedback and exploration of Si Hall probe microscopy at elevated temperatures with both methods of feedback.

Fig. 11 shows a magnetic image of HDD sample obtained in AFM tracking mode from 25°C to 150°C with a scanning speed of 5µm/s, the pixel size of 256 × 256 and a scan area of 50µm × 50µm.

The results are shown in Fig. 11 confirm the success of AFM feedback tracking system with micro-Hall probes up to 150°C. From the line cross section of these images as shown in the middle, it can

be observed that the distortions in the scanned images increase by increasing the temperature of the sample. It can be correlated with two factors;

1) The deterioration of the scanned image can partially be correlated with an increase in the noise level of Hall signal due to an increase in the temperature. This mainly due to decrease in V_H (1) by increasing the temperature of thin film, which is produced from thinning of Si device layer by reactive ion etching, there is an increase in the number of carrier, n , which is mainly due to de-trapping from the trapping centers.

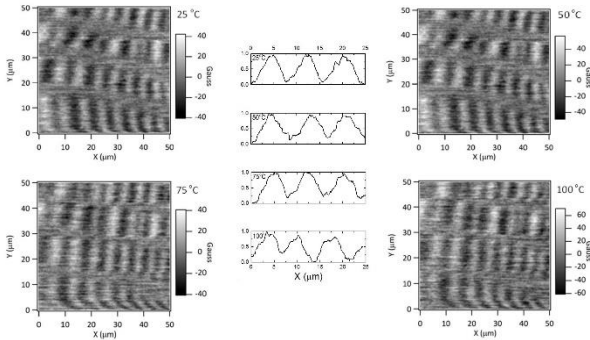


Fig. 11: SHPM image of hard disc sample at high temperatures, 25°C – 150°C using QTF AFM feedback. Scanning speed was 5 μ m/s

2) The deterioration of the scanned image can partially be correlated with an increase in the noise level of Hall signal due to an increase in the temperature. This mainly due to decrease in V_H (1) by increasing the temperature of thin film, which is produced from thinning of Si device layer by reactive ion etching, there is an increase in the number of carrier, n , which is mainly due to de-trapping from the trapping centers.

3) As shown in Fig. 10, by increasing the temperature the resonance frequency and quality factor of the quartz crystal tuning fork is also affected due to the softness of the glue a) used to fix one prong of the QTF with PCB b) Hall sensor chip on QTF and effect of temperature on the properties of QTF material. However, this change is still much less than the conventional silicon AFM cantilevers. Further investigation is under process to find out the methods to improve the thermal stability of the QTF AFM feedback and exploration of Si Hall probe microscopy at elevated temperatures with both methods.

3.3. Comparison with other probes

Table 1 reports the characteristics of three micro-Hall cross-sensors at 300K fabricated in same class 100 clean room environments by the group using optical lithography techniques. The current related sensitivity is computed using (3) by considering 100 μ A as bias current specified in the reference, not necessarily equal to the maximum current possible.

Electrical and Magnetic characteristics of these three different types of Hall probes show that GaN to be a better choice due to its high sensitivity while PHEMT and Si HPs are comparable with an advantage to Si as its fabrication process is CMOS compatibility. The image quality of SHPM scans at 150oC shows that due to its better physical strength and high band gap, GaN is far better than Si while in contract PHEMT even did not produce an image at 50oC with the present system while at low-temperature PHEMT is much better than the other two choices. Ultimate temperature limits for GaN or Si has not been probed, as the system was not able to work at higher temperatures. Therefore, the choice of material for fabrication of HP depends on its operation and application.

4. Conclusion

Micro-Hall probes with a Hall cross-area of 0.7 μ m \times 0.7 μ m with an optimized thickness of Si device layer (510nm) were fabricated and implemented in the variable temperature magnetic imaging system. These Hall probes have been integrated in scanning Hall probe microscopy using STM or quartz tuning fork (QTF) AFM interchangeable feedback configurations. In this study QTF has been adopted over cantilever as they are readily available and the force sensing is performed using the simple current to voltage converter, they provide a cheap solution compared to cantilever approach.

To quantify the scanning results hard disc sample has been scanned using same scan parameters at all temperatures. It has been observed that at low temperatures STM tracking mode dominates QTF-AFM tracking while at room temperatures both are of comparable quality. At high temperatures STM tracking feedback based SHPM failed to operate due to two main facts; the degradation of the sample as it was coated with a conductive material and secondly the evaporated STM tip has been peeled off due to poor adhesion at the corner of the Hall sensor chip.

Furthermore, by increasing the temperature leakage current between STM tip and Hall probe masks the Hall signal and it limits the use at elevated temperatures. Application of Si Hall sensors coupled with Quartz crystal tuning fork as AFM feedback in SHPM of hard disc samples has been successfully demonstrated for a temperature range of 25°C – 150°C. QTF method has been found to provide better lifetime performance for Si Hall sensors than STM trucking mode. In comparison with SHPM with GaN and PHEMT Hall sensors, Si Hall sensor with QTF-AFM tracking SHPM exhibit same working range as for GaN for high temperatures and for low temperatures it is comparable with PHEMT. Secondly, in the presented method of coupling Si Hall sensor with QTF makes it possible to have switchable feedback configuration to STM or AFM, if tip coated Hall chip is used, for variable temperature applications.

Table 1: Comparison of imaging capability of different Hall Effect sensors fabricated under same conditions with their critical parameters of interest

Type → Parameters:	GaAs/ AlGaAs (PHEMT)	GaN/AlGaN (2DEG)	SOI
Reference:	(Akram et al., 2009)	(Akram et al., 2008)	This work
n_s (cm ⁻²):	6.25×10^{12}	6.3×10^{12}	2.2×10^{14}
T_{eff} (nm):	10	18	410
R_s (K Ω):	12	12	30
R_H (m Ω /G):	5	10	4.31
S_I (VA ⁻¹ T ⁻¹):	50	100	49.4
B_{min} (mG/Hz) @ 1kHz:	70.5	35	112

SHPM Scan using AFM tracking feedback

Acknowledgment

This work is supported in Turkey by TÜBİTAK, Project Numbers: TBAG-(105T473), TBAG-(105T224). The author is thankful to Nano Magnetics Instruments Ltd, for technical support and guidance in completing the experiments. The Experimentation was done at advance research lab of Bilkent University in collaboration with Nanomagnetism Instruments Ltd.

References

- Abderrahmane A, Koide S, Sato SI, Ohshima T, Sandhu A, and Okada H (2012). Robust Hall effect magnetic field sensors for operation at high temperatures and in harsh radiation environments. *IEEE Transactions on Magnetics*, 48(11): 4421-4423.
- Akram R, Dede M, and Oral A (2008). Variable temperature-scanning Hall probe microscopy with GaN/AlGaN two-dimensional electron gas (2DEG) micro Hall sensors in 4.2–425 K range using novel quartz tuning fork AFM feedback. *IEEE Transactions on Magnetics*, 44(11): 3255-3260.
- Akram R, Dede M, and Oral A (2009). Imaging capability of pseudomorphic high electron mobility transistors, Al Ga N/GaN, and Si micro-Hall probes for scanning Hall probe microscopy between 25 and 125° C. *Journal of Vacuum Science and Technology B: Microelectronics and Nanometer Structures Processing, Measurement, and Phenomena*, 27(2): 1006-1010.
- Akram R, Fardmanesh M, Schubert J, Zander W, Banzet M, Lomparski D, and Krause HJ (2006). Signal enhancement techniques for rf SQUID based magnetic imaging systems. *Superconductor Science and Technology*, 19(8): 821-824.
- Bellekom S and Sarro PM (1998). Offset reduction of Hall plates in three different crystal planes. *Sensors and Actuators A-Physical*, 66(1-3): 23-28.
- Besse PA, Boero G, Demierre M, Pott V, and Popovic R (2002). Detection of a single magnetic microbead using a miniaturized silicon Hall sensor. *Applied Physics Letters*, 80(22): 4199-4201.
- Betzig E, Trautman JK, Wolfe R, Gyorgy EM, Finn PL, Kryder MH, and Chang CH (1992). Near-field magneto-optics and high density storage. *Optics and Photonics News.*, 3(12): 24-25.
- Blagojevic M, Kayal M, and De Venuto D (2006a). FD SOI Hall sensor electronics interfaces for energy measurement. *Microelectronics Journal*, 37(12): 1576-1583.
- Blagojevic M, Kayal M, Gervais M, and De Venuto D (2006b). SOI hall-sensor front end for energy measurement. *IEEE Sensors Journal*, 6(4): 1016-1021.
- Boero G, Demierre M, and Popovic RS (2003). Micro-Hall devices: Performance, technologies and applications. *Sensors and Actuators A: Physical*, 106(1-3): 314-320.
- Boero G, Utke I, Bret T, Quack N, Todorova M, Mouaziz S, and Hoffmann P (2005). Submicrometer Hall devices fabricated by focused electron-beam-induced deposition. *Applied Physics Letters*, 86(4): 042503. <https://doi.org/10.1063/1.1856134>
- Chong BK, Zhou H, Mills G, Donaldson L, and Weaver JMR (2001). Scanning Hall probe microscopy on an atomic force microscope tip. *Journal of Vacuum Science and Technology A: Vacuum, Surfaces, and Films*, 19(4): 1769-1772.
- Chung GS (1993). Thin SOI structures for sensing and integrated-circuit applications. *Sensors and Actuators A-Physical*, 39(3): 241-251.
- Gruger H, Vogel U, and Ulbricht S (2006). Setup and capability of CMOS Hall sensor arrays. *Sensors and Actuators A-Physical*, 129(1-2): 100-102.
- Guethner P, Fischer U, and Dransfeld K (1989). Scanning near field acoustic microscopy. *Applied Physics B*, 48(1): 89-92.
- Julian S (2014). Scanning probe microscopy from the perspective of the sensor. Ph.D. Dissertation, University of Nottingham, Nottingham, UK.
- Karci O, Piatek OJ, Jorba P, Dede M, Rønnow MH, and Oral A (2014). An ultra-low temperature scanning Hall probe microscope for magnetic imaging below 40 mK. *Review of Scientific Instruments*, 85(10): 103703.
- Kejik P, Boero G, Demierre M, and Popovic RS (2006). An integrated micro-Hall probe for scanning magnetic microscopy. *Sensors and Actuators A: Physical*, 129(1-2): 212-215.
- Kirtley JR and Wikswo JP (1999). Scanning SQUID microscopy. *Annual Review of Materials Science*, 29(1): 117-148.
- Kumagai Y, Abe M, Sakamoto S, Handa H, and Sandhu A (2008). Sensitivity dependence of Hall biosensor arrays with the position of superparamagnetic beads on their active regions. *Journal of Applied Physics*, 103(7): 07A309. <https://doi.org/10.1063/1.2833306>

- Kunets VP, Black WT, Mazur YI, Guzun D, Salamo GJ, Goel N, and Santos MB (2005). Highly sensitive micro-Hall devices based on Al 0.12 In 0.88 Sb/ In Sb heterostructures. *Journal of Applied Physics*, 98(1): 014506. <https://doi.org/10.1063/1.1954867>
- Lyu F, Zhang Z, Toh EH, Liu X, Ding Y, Pan Y, Li C, Li L, Sha J, and Pan H (2015). Performance comparison of cross like hall plates with different covering layers. *Sensors*, 15(1): 672-686.
- Martin Y and Wickramasinghe HK (1987). Magnetic imaging by "force microscopy" with 1000 Å resolution. *Applied Physics Letters*, 50(20): 1455-1457.
- Mihajlović G, Xiong P, Monár SV, Ohtani K, Ohno H, Field M, and Sullivan GJ (2005). Detection of single magnetic bead for biological applications using an InAs quantum-well micro-Hall sensor. *Applied Physics Letters*, 87(11): 112502. <https://doi.org/10.1063/1.2043238>
- Oral A, Bending SJ, and Henini M (1996). Real-time scanning hall probe microscopy. *Applied Physics Letters*, 69(9): 1324-1326.
- Paun M, Sallese JM, and Kayal M (2013a). Temperature considerations on Hall Effect sensors current-related sensitivity behavior. *Analog Integrated Circuits and Signal Processing*, 77(3): 355-364.
- Paun MA (2016). Main parameters characterization of bulk cmos cross-like hall structures. *Advances in Materials Science and Engineering*, 2016: Article ID 6279162, 7 pages. <https://doi.org/10.1155/2016/6279162>
- Paun MA, Sallese JM, and Kayal M (2010). Geometry influence on Hall effect devices performance. *UPB Science Bull*, 72(4): 257-271.
- Paun MA, Sallese JM, and Kayal M (2013b). Comparative study on the performance of five different Hall effect devices. *Sensors*, 13(2): 2093-2112.
- Paun MA, Sallese JM, and Kayal M (2014). Evaluation of characteristic parameters for high performance hall cells. *Microelectronics Journal*, 45(9): 1194-1201.
- Popovic RS (2004). *Hall Effect Devices*. 2nd Edition, Institute of Physics Publishing, Bristol, UK.
- Sandhu A, Kurosawa K, Dede M, and Oral A (2004). 50 nm Hall sensors for room temperature scanning Hall probe microscopy. *Japanese Journal of Applied Physics*, 43(2R): 777-778.
- Schmidt F and Hubert A (1986). Domain observations on CoCr-layers with a digitally enhanced Kerr-microscope. *Journal of magnetism and magnetic materials*, 61(3): 307-320.
- Schweinböck T, Weiss D, Lipinski M, and Eberl K (2000). Scanning Hall probe microscopy with shear force distance control. *Journal of Applied Physics*, 87(9): 6496-6498.
- Xiao-Fen Li, Mehdi K, Goran M, and Venkat S (2016). Critical current density measurement of striated multifilament-coated conductors using a scanning Hall probe microscope. *Superconductor Science, and Technology*, 29(8): 085014. <https://doi.org/10.1088/0953-2048/29/8/085014>
- Xu Y and Pan H. B (2011). An improved equivalent simulation model for CMOS integrated Hall Plates. *Sensors*, 11(6): 6284-6296.
- Yamamura T, Nakamura D, Higashiwaki M, Matsui T, and Sandhu A (2006). High sensitivity and quantitative magnetic field measurements at 600 C. *Journal of Applied Physics*, 99(8): 08B302. <https://doi.org/10.1063/1.2158693>